ACS APPLIED MATERIALS & INTERFACES

Research Article

www.acsami.org

Receptor-Mediated Liposome Fusion Kinetics at Aqueous/Liquid Crystal Interfaces

Katherine M. Macri, Patrick S. Noonan, and Daniel K. Schwartz*

Department of Chemical and Biological Engineering, University of Colorado Boulder, Boulder, Colorado 80309-0596, United States

ABSTRACT: Membrane fusion events are essential to cell biology, and a number of reductionist systems have been developed to mimic the behavior of these biological motifs. One such system monitors the DNA hybridization-mediated fusion of liposomes with the liquid crystal (LC) interface by observing changes in LC orientation using a simple optical detection scheme. We have systematically explored key parameters of this system to determine their effects on individual elementary steps of the complex fusion mechanism. The liposome composition, specifically the degree of lipid unsaturation and PE content, decreased the bilayer rigidity, thereby increasing the rate of vesicle rupture under the stress applied by DNA hybridization. In contrast, the presence of cholesterol had the opposite effect on the mechanical properties of the bilayer, and hence of the membrane fusion rates. The accessibility of receptor moieties (i.e., complementary DNA oligonucleotides) affected the fusion kinetics by modulating the rate of hybridization events. DNA accessibility was controlled by systematic variation of the length of the DNA receptor molecules and the thickness of the steric barrier comprised of adsorbed PEGylated lipids. These results provide design rules for understanding the trade-offs between response kinetics and other important system properties, such as nonspecific adsorption. Moreover, these findings improve our understanding of the biophysical properties of membrane fusion, an important process in both natural and model systems used for bioassay and bioimaging applications.

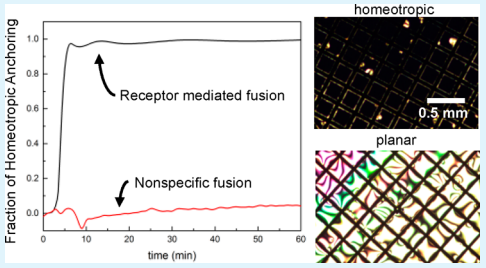

KEYWORDS: *liposome fusion, lipid composition, sensor, DNA, liquid crystal*

INTRODUCTION

Vesicle fusion plays a critical role in cell biology. For example, reproduction and development,[1] intracellular trafficking,[2] mitochondrial fusion,[3] and viral entry,[4] all involve fusion processes that are governed by a diverse set of proteins. Despite this diversity, the mechanism of vesicle fusion appears to be conserved; proteins bring two membranes into close proximity and a local disruption of bilayer structure leads to the formation of an intermediate hemifused state that can transition to a fusion pore. A number of artificial systems have been designed to mimic cellular fusion machinery in order to gain insight into the biophysical mechanics of selective bilayer fusion.[5,6] Many of these systems are able to monitor individual fusion events using both SNARE protein machinery[7,8] and artificial mimics[9−11] as receptors. Although some relevance to biological systems is lost with these reductionist platforms, they allow us to study the fundamental process of membrane fusion at a mechanistic level. Moreover, systems that enable programmed membrane fusion have been proposed for applications associated with bio-assays,[12] bioimaging contrast agents,[13] and targeted drug delivery.[14,15]

In the studies outlined here we take advantage of the unique properties of liquid crystals (LCs) to study vesicle fusion at the aqueous/liquid crystal interface. Liquid crystalline materials afford a unique way to study interfacial phenomena because of their dynamic and responsive properties,[16] their long-range molecular order, and the broken symmetries associated with LC phases, which lead to distinctive optical properties, for example, optical anisotropy (i.e., birefringence).[17] The ordering of LC mesogens at interfaces can be controlled through a number of chemical and physical processes, and because these molecules possess long-range orientational order, alignment at the interface propagates over macroscopic length scales, providing an intrinsic amplification mechanism. Surface interactions are therefore an important tool to control LC alignment, which is readily detected using polarized light. The long axis of molecules within an LC material can be aligned parallel to the surface normal (so-called homeotropic anchoring) by a layer of long-chain aliphatic hydrocarbons such as a self-assembled monolayer (SAM) or an adsorbed surfactant/lipid layer.[18,19] On the other hand, direct contact between an LC material and an aqueous phase induces planar anchoring (i.e., alignment of the molecular axis within the surface plane). These phenomena have led to a convenient experimental realization, wherein a layer of LC material is sandwiched between a SAM-coated solid surface and an aqueous phase, creating a "hybrid nematic cell" that is birefringent.[20] A number of studies have explored the detailed and complex effects of surfactants at the aqueous LC interface,[21−25] including the spontaneous adsorption of phospholipid vesicles from solution.[26,27] LC realignment at the aqueous interface is generally observed above a threshold concentration of surfactant molecules

Received: July 14, 2015
Accepted: August 28, 2015
Published: August 28, 2015

DOI: 10.1021/acsami.5b06351
ACS Appl. Mater. Interfaces 2015, 7, 20400−20409

containing linear alkyl chains, shifting the anchoring from planar to homeotropic and eliminating the optical birefringence of the sample. LCs are therefore an intriguing platform for label-free sensing, because the long-range orientational response to surface interactions allows for high sensitivity and the optical anisotropy permits convenient detection of alignment with polarized light.

We previously reported a system to detect receptor-mediated liposome fusion events using LCs as a transducing element.[12] This system employed a PEG-functionalized lipid layer that sterically inhibited spontaneous liposome fusion in the absence of specific receptor-binding events. Complementary DNA receptor moieties present both in liposomes and at the interface induced liposome rupture and fusion, resulting in an optically detectable LC reorientation event. By incorporating an aptamer as part of this scheme, we found that the system provided a sensitive and specific response to a particular protein analyte. In this work, we study the underpinning mechanism of liposome fusion with the LC interface. In particular, we explored the effect of lipid composition on the mechanical properties of the bilayer and how the accessibility of receptor moieties influenced fusion rates. Moreover, the results reported here provide insights into the process of programmed vesicle fusion, a critical step in several drug delivery/bioassay systems.

Here, we aimed to understand the microscopic mechanisms underlying the macroscopic response, by systematically exploring the relevant parameters that govern LC realignment due to receptor-mediated liposome fusion. We postulated that the liposome fusion mechanism occurs in three distinct steps (Figure 1): (1) liposomes adsorb from solution to the steric

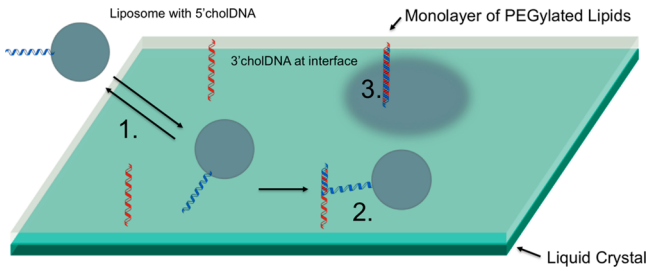

Figure 1. Schematic of the mechanism of liposome fusion with a liquid crystal interface. (1) Liposomes nonspecifically adsorb to a PEG-lipid layer, which serves as a steric barrier for spontaneous fusion, where they can diffuse laterally or desorb back into solution. (2) DNA hybridization events initiate the liposome fusion process by (3) creating strain within the bilayer, leading to vesicle rupture and fusion.

PEG-barrier, (2) DNA hybridization events tether the liposome to the interface and induce strain on the bilayer, and (3) the exposed lipid tails interact with the hydrophobic liquid crystal material, triggering vesicle rupture and fusion. We hypothesized that these elementary steps could be isolated by systematically varying system parameters that separately influenced the tethering process or the fusion process, respectively. Specifically, we studied the effects of modifying (1) the receptor accessibility or (2) the mechanical properties of the lipid bilayer on the overall fusion kinetics of the system, relative to the kinetics in control experiments in the absence of functional receptors. These parameters likely influenced one of two steps in the fusion mechanism: the recognition event that brought liposomes into close contact with the LC interface, or liposome rupture as a function of applied stress. Improving our understanding of the biophysical properties that contribute to membrane fusion is important for the design of new and better fusogenic systems for drug delivery, transfection, and sensing platforms.

MATERIALS AND METHODS

Lipids (1,2-dipalmitoyl-*sn*-glycero-3-phosphocholine (DPPC), 1,2-dioleoyl-*sn*-glycero-3-phosphocholine (DOPC), 1,2-dioleoyl-*sn*-glycero-3-phosphoethanolamine (DOPE), 1,2-distearoyl-*sn*-glycero-3-phosphoethanolamine-*N*-[methoxy(polyethylene glycol)-1000] (ammonium salt) (DSPE-PEG1k), 1,2-distearoyl-*sn*-glycero-3-phosphoethanolamine-*N*-[methoxy (polyethylene glycol)-2000] (ammonium salt) (DSPE-PEG2k), 1,2-distearoyl- sn-glycero-3-phosphoethanolamine-N-[methoxy-(polyethylene glycol)-5000] (ammonium salt) (DSPE-PEG5k) were purchased from Avanti Polar Lipids, Inc. Cholesterol (CH) was purchased from Sigma-Aldrich. Oligonucleotides (Table 1) modified with a cholesterol-TEG linker were purchased from IDT Technologies. The liquid crystal used in this study was E7 (Merck, Ltd.), a mixture of three cyanobiphenyl compounds and one cyanotriphenyl with a nematic−isotropic transition temperature T_{NI} = 58 °C.

Liposomes were prepared by first mixing a fixed quantity of lipids dissolved in chloroform in a small test tube. The relative fractions of lipids varied according to the parameters for each experiment as detailed below. The chloroform was evaporated using a stream of nitrogen, leaving a lipid film. The lipid film was hydrated with an aqueous buffer (1× PBS, pH 7.4, Life Technologies), vortexed for 30 s, followed by sonication for 1 h. The suspension was then diluted to a concentration of 5 mM and cholesterol-modified DNA (cholDNA) was added to achieve a 1:2500 DNA/lipid ratio. This mixture was stirred for 1 h at room temperature to allow the cholDNA to incorporate into the liposomes. LUVs (large unilamellar vesicles) were achieved by the extrusion method. The lipid mixture was extruded 11 times by hand through a 0.05 μm polycarbonate filter (Whatman) to achieve a uniform size distribution. Vesicle diameter was consistently measured at 125 nm using dynamic light scattering. All liposomes were used within 48 h of preparation. DSPE-PEG micelles were prepared by dissolving the PEGylated lipid in buffer (1× PBS, pH 7.4) and adding 3′cholDNA (when applicable) to achieve a final concentration of 40.2 μM DSPE-PEG and 0.85 μM 3′cholDNA. The mixture was vortexed for 30−60 s to incorporate cholDNA into the micelles and used within 24 h.

Each experimental system, comprising a stabilized LC layer and the contacting solution, was housed in a silicone well placed on top of a glass slide. Glass microscope slides modified with a self-assembled monolayer of octadecyltriethoxysilane (OTES) were prepared according to published procedures.[18] Slides were rinsed with a 2% Micro90 solution, deionized water, and isopropanol, and dried with a stream of N_2. The substrate was immersed in warm piranha solution (30% aqueous H_2O_2 (Fisher Scientific) and concentrated H_2SO_4 (Fisher Scientific) 1:3, v/v) (*Caution: piranha reacts strongly with organic compounds and should be handled with extreme caution; do not store in a closed container*) for 1 h, followed by a rinse with deionized water (18.2 MΩ) and a 1 h UV-ozone treatment. Clean slides were added to a deposition solution containing *n*-butylamine and OTES in toluene and incubated for 1 h at 60 °C. Upon removal, slides were rinsed with toluene and dried under a stream of N_2. The water contact angle was measured using a custom-built goniometer and observed to be >95°, consistent with monolayer coverage of the OTES substrate.

DOI: 10.1021/acsami.5b06351
ACS Appl. Mater. Interfaces 2015, 7, 20400−20409

Table 1. DNA Oligonucleotide Sequences

name	sequence
3′1CHOL-AC10	5′ ACA ACC AAC A 3′-CHOL
5′CHOL-TG10	CHOL-5′ TGT TGG TTG T 3′
3′CHOL-AC20	5′ ACA ACC AAC ACA CAA ACA AC 3′-CHOL
5′CHOL-TG20	CHOL-5′ GTT GTT TGT GTG TTG GTT GT 3′
3′CHOL-AC30	5′ ACA ACC AAC ACA CAA ACA ACC AAC ACA CAA 3″-CHOL
5′CHOL-TG30	CHOL-5′ TTG TGT GTT GGT TGT TTG TGT GTT GGT TGT 3′
3′CHOL-AC40	5′ ACA ACC AAC ACA CAA ACA ACC AAC ACA CAA ACA ACC AAC A 3′-CHOL
5′CHOL-TG40	CHOL-5′ TGT TGG TTG TTT GTG TGT TGG TTG TTT GTG TGT TGG TTG T 3′
3′CHOL-AC50	5′ ACA ACC AAC ACA CAA ACA ACC AAC ACA CAA ACA ACC AAC ACA CAA ACA AC 3′-CH
5′CHOL-TG50	CHOL-5′ GTT GTT TGT GTG TTG GTT GTT TGT GTG TTG GTT GTT TGT GTG TTG GTT GT 3′
3′CHOL-Thr	5′ GTT GGT TTT GGA CAT CAG AAA TAA GGC ACG ACG GA 3′-CHOL
5′CHOL-Thr	CHOL-5′ TCC GTC GTG CCT TAT TTC TGA TGT CCA AAA CCA ACC ACA 3′
CS-Thr	5′ GGT TGG TGT GGT TGG TTT 3′

Slides were stored at room temperature in a vacuum desiccator and used within 3 weeks.

LC films were created by housing the nematic LC within an electron microscopy (EM) grid placed on an OTES-functionalized glass slide. Grids were placed inside silicone wells and ∼0.25 μL E7 was added to each grid. Excess LC was removed via capillary action, and the sample was heated above the isotropic transition temperature (T_{NI} = 58 °C) and allowed to cool to room temperature. Silicone dividers placed on top of the substrate created a ∼25 μL well to contain the sample. All species were introduced to the aqueous-LC interface through an aqueous phase added to the silicone well above the LC film. Liposome fusion experiments were carried out in two steps. In the first step, two 25 μL aliquots of an aqueous solution containing DSPE-PEG micelles were added to the silicone well housing the LC film. The second aliquot was removed to create a planar interface with the air and prevent curvature of the aqueous phase from distorting polarized light images. The PEGylated lipids adsorbed to the liquid crystal interface creating a stable, planar interface that blocked nonspecific adsorption of additional phospholipids. The buffer was then exchanged five times by adding an additional 25 μL of buffer to the aqueous phase, pipetting to mix the contents of the well, then removing 25 μL to reestablish a planar interface. For all experiments, liposomes were then added to the aqueous phase in step two, 3 min after the initial introduction of DSPE-PEG micelles. As with the buffer exchange, 25 μL of the desired liposome solution was added to the well, pipetted up and down to mix the contents, and removed to maintain a planar air−water interface. The effect of liposome fusion at the interface was observed by monitoring LC alignment using polarized light microscopy (PLM).

Images of the LC film were captured by placing the sample between crossed polarizers of a custom-built optical microscope. PLM images were analyzed using a custom Mathematica code. The EM grid afforded a uniform LC film size, making it easy to compare images between samples. ImageJ was used to crop the background from each image leaving only the LC film present in the grid to be analyzed. Each image was binarized to determine the number of dark pixels, correlating to homeotropic domains in the LC film. A planar interface inherently contains some optical extinction leading to the appearance of dark brushes. We normalized our images to account for this phenomenon when observing the formation of homeotropic domains and defined the fractional change in homeotropic anchoring (Δf_H) using the following equation:

$$\Delta f_H = \frac{f_t - f_0}{\overline{f_H} - f_0}$$

where f_0 was the fraction of dark pixels in a planar LC film and f_t was the fraction of dark pixels at time t. $\overline{f_H}$ was a constant that represented the average value of the fraction of dark pixels in a set of nominally homeotropic images. The effective rate constant (k_H) for liposome fusion was defined as the inverse of the time interval necessary for a LC film to reach 50% homeotropic coverage after the addition of liposomes.

RESULTS AND DISCUSSION

In this study, we examined the variables that govern receptor-mediated liposome fusion at the aqueous-liquid crystal interface. The spontaneous fusion of liposomes was inhibited by the deposition of a monolayer of PEGylated lipids at the LC interface, creating a steric barrier to fusion.

These PEGylated lipids created a monolayer of loosely packed PEG moieties (controlled by repulsive PEG−PEG interactions) at a low packing density. For PEG1000, using a simple polymer brush model of the surface for grafted polymers,[28] we estimated the packing density (σ) to be between 0.68 molecules/nm^2 (for overlapping polymers) and 0.17 molecules/nm^2 (for noninteracting polymers) using the following equation:

$$\sigma = \frac{1}{D^2}$$

where D is the mean distance between two PEG grafts. D was defined as $D = R_g$ for overlapping polymers and $D = 2R_g$ for noninteracting polymers. The packing densities for larger PEG moieties are estimated at 0.30−0.08 molecules/nm^2 for PEG2000 and 0.10−0.026 for PEG5000. Although these values represent rough estimates of the packing density of PEG lipids, we note that are all well below the threshold lipid concentration required to achieve homeotropic anchoring of the nematic LC (∼1.8 lipids/nm^2).[29]

In a subsequent step, liposomes functionalized with DNA receptor molecules hybridized with complementary DNA at the LC interface. Under appropriate conditions, this receptor binding permitted the liposome to overcome the steric barrier and fuse with the lipid monolayer at the LC interface. Importantly, to induce fusion, the DNA receptors in the liposome and at the LC interface were required to hybridize in the cis geometry, where the outer ends of the DNA strands in

DOI: 10.1021/acsami.5b06351
ACS Appl. Mater. Interfaces 2015, 7, 20400−20409

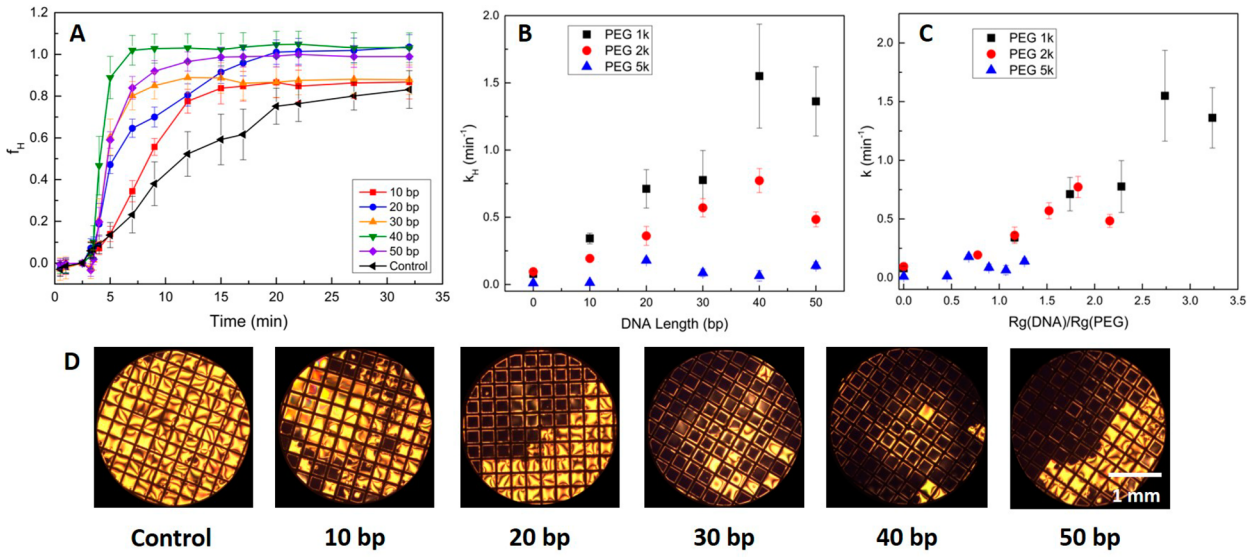

Figure 2. Effect of DNA oligonucleotide length on the rate of LC realignment. (A) The fractional coverage of homeotropic anchoring observed with complementary cholDNA of different lengths. PEG2000 was used to create a steric barrier at the interface. (B) The effective rate constant (k_H) as a function of DNA oligomer length for various PEG headgroups. A DNA length of 0 base pairs indicates the nonspecific fusion events for each set of data. Error bars represent the standard error of each data set. (C) Vesicle fusion rate as a function of the ratio of R_g(DNA)/R_g(PEG). (D) Polarized light microscopy images of the LC interface 4 min after the introduction of liposomes. PEG2000 was present at the interface, and the control experiment did not contain DNA (nonspecific fusion).

the opposing layers were complementary.[12] In this geometry, hybridization brought the liposome into contact with the LC interface, inducing mechanical stress that promoted liposome rupture.[10,30] Each fusion event deposited a large number of phospholipids at the interface, creating a saturated monolayer and realigning the bulk LC sample. We observed what appeared to be a single cooperative phase transition across the sample once a threshold lipid concentration was reached. Although lateral demixing events have been observed by our group[25] and others[31] in related systems, we did not observe macroscopic phase separation on length scales accessible to the polarized microscope.

It is important to note that because we observed fusion indirectly, we can only speculate as to the number of hybridization events needed to induce fusion of a single liposome. One study suggested that liposome fusion with a supported lipid bilayer can occur as the result of a single hybridization event; however the kinetics of the docking step were greatly reduced compared to systems that enabled multiple hybridization events.[32] In addition, previous work on this system by our lab reported an increase in fusion kinetics with a greater number of DNA receptors.[12] These observations suggest that while a single hybridization event may be sufficient to induce fusion, increasing the number of receptors results in more rapid docking and/or fusion kinetics. However, we cannot distinguish if vesicles fuse immediately upon the first hybridization event or whether this first event holds the vesicle in place allowing additional hybridization events to strain the bilayer and promote fusion.

This phenomenon has a number of applications, including the optimization of a highly sensitive liquid crystal based sensor, as well as an improved mechanistic understanding of liposome fusion with a hydrophobic interface. A viable receptor-mediated sensing platform requires a rapid detection scheme when the target is present, along with high sensitivity and low background levels. Therefore, we require fast receptor-mediated fusion kinetics, with a low rate of nonspecific fusion. As a general rule of thumb, a fusion rate constant (k_H) greater than 0.2 min^{-1}, indicating 50% homeotropic coverage after a 5 min incubation time, coupled with a large ratio of DNA-induced to nonspecific fusion rates (>10) represent appropriate conditions for the aforementioned sensing applications.

As described above, we focused on variables that would allow us to isolate the effects of the receptor binding and liposome fusion events, respectively. To probe the receptor binding step, we controlled the accessibility of DNA at the LC interface by varying the length of DNA receptor moieties in conjunction with the molecular weight of the PEG headgroup (which formed the steric barrier). On the other hand, to probe the kinetics of the liposome fusion events, we varied the lipid composition of the liposomes, which is known to influence the mechanical properties of the bilayer, altering the fluidity and bending modulus of the liposome. In particular, we hypothesized that upon DNA hybridization-induced stress, these mechanical properties would modulate the rate at which vesicle rupture occurred.

Effects of DNA Accessibility on Liposome Fusion Kinetics. In the context of a detection platform, nonspecific liposome fusion events represent a background response that must be minimized to achieve high sensitivity. This was accomplished by loading the LC-aqueous interface with a PEG-lipid monolayer, where the PEG chains formed a polymer brush layer that resisted liposome fusion. The repulsive lateral PEG–PEG steric interactions within the interfacial layer led to a situation where the lipid tails achieved only a relatively low packing density, enabling the LC phase to remain in a planar orientation.[31] Stochastic liposome fusion events, either non-specific or receptor-mediated, deposited additional lipids at the interface, eventually causing LC reorientation, which represented the transduced "signal". Thus, one goal of these experiments was to identify conditions where receptor-mediated fusion was rapid and nonspecific fusion was minimal.

We hypothesized that following an initial adsorption step, where a liposome from solution nonspecifically adsorbed to the

DOI: 10.1021/acsami.5b06351
ACS Appl. Mater. Interfaces 2015, 7, 20400–20409

PEG brush, a DNA-mediated docking event escorts the liposome through the steric barrier and into contact with the interface. As described above, this involves cis DNA hybridization between DNA strands in the liposome and at the LC interface, respectively. In this cis geometry, we expect that the exposed ends of the DNA strands will hybridize first, followed by a "zippering up" process that exerts increasing force on the liposome. If this picture is correct, it seems likely that the kinetics of the docking step should depend on the accessibility of the termini of the complementary DNA oligonucleotides. For example, if the DNA at the LC interface were completely buried within the PEG brush layer, hybridization events would be rare, leading to slow overall fusion kinetics, whereas the fusion kinetics would be faster if the DNA extended beyond the PEG brush. This phenomenology is confirmed in Figures 2A and 2D, which compare DNA receptors of various lengths in the presence of a PEG2000 steric layer comprised of PEG molecules with a free radius of gyration R_g = 1.8 nm.[33] The fusion rate for liposomes displaying 10-nucleotide DNA, with a radius of gyration of $R_g \approx 1.4$ nm[34] was only marginally faster than that in control experiments without receptor DNA. However, the fusion rate increased significantly for DNA chains with 20 and 30 nucleotides ($R_g \approx 2.1$ and 2.7 nm respectively), which were significantly larger than the PEG chains. To understand these phenomena, we systematically explored the effects of DNA length and the thickness of the PEG brush layer on the rate of liposome fusion.

Liposomes were prepared with a 2:1:1 DOPC/DOPE/CH molar ratio and the length of 5′cholDNA was systematically varied from 10−50 nucleotides (5′CHOL-TG10-50, Table 1). The 3′cholDNA at the LC interface contained a complementary sequence of the same length. Each sequence contained only A/C or T/G nucleotides to prevent secondary structure from affecting fusion dynamics. Two distinct trends were clearly observed, illustrating the effects of DNA and PEG molecular size, respectively. As shown in Figures 2A and 2B, we observed a general increase in the rate of liposome fusion as the length of the DNA strands increased. Moreover, for a given length of DNA, shorter PEG headgroups led to overall faster fusion rates (Figure 2B). Fusion was almost completely inhibited when DNA receptors were short (10 bp) and the steric barrier was large (PEG5000 g/mol), supporting our hypothesis that DNA accessibility played an important role in modulating fusion kinetics. However, this was not the only effect of changing the thickness of the PEG brush, because nonspecific fusion events decreased with increasing PEG headgroup size, as illustrated by the rates of the control experiments (0 DNA length in Figure 2B). For example, in the presence of a PEG2000 steric barrier, nonspecific fusion led to significant homeotropic coverage over a 5−10 min period, with PEG5000 no change in LC realignment was observed (in the absence of DNA receptors) even after a 2-h incubation time. Thus, the thickness of the PEG brush appeared to have two distinct effects, in that it influenced the intrinsic rate of liposome fusion (evident in the effect in control experiments without receptor DNA) and also affected the accessibility of DNA. To emphasize the importance of the relative sizes of DNA and PEG length on DNA accessibility, we plotted the fusion rate versus the ratio of the radii of gyration of the ssDNA strand to that of the PEG constituent of the steric brush, R_g(DNA)/R_g(PEG). As shown in Figure 2C, these data suggest that the fusion rate did not increase significantly above background levels until the length of the DNA receptor was increased such that the ratio R_g(DNA)/R_g(PEG) > 1. We emphasize that we are not suggesting that the radius of gyration of PEG or DNA directly reflects the physical dimension of the interfacial layer in these experiments; but in the absence of more detailed information about the interfacial structure, the ratio R_g(DNA)/R_g(PEG) represents a reasonable parameter to describe the relative sizes of the two molecules.

The kinetics of DNA hybridization has been thoroughly characterized[35] and is generally accepted to proceed through a nucleation complex, followed by a "zippering-up" of the remaining base pairs.[36−38] The rate-determining step is the formation of the nucleation complex, which consists of stable intermolecular base pairing a few nucleotides in length.[36] When confined to a surface, the rate of hybridization becomes dependent on a number of other factors including probe density and length, surface heterogeneity, and nonspecific adsorption.[39−41] This general picture suggests that when the brush layer is thick (DSPE-PEG5000 g/mol) short DNA oligonucleotides will not penetrate significantly beyond the PEG-chains at the interface, reducing or completely inhibiting the number of nucleation events. One would therefore expect to observe a systematic increase in fusion rates with DNA receptor length, due to the increased accessibility of interfacial DNA beyond the steric barrier, coupled with the larger association constant (K_a) for longer DNA oligonucleotides.[42] We note that there may be an ideal length for the DNA receptor strands that is long enough to penetrate the steric barrier, has a low rate of dissociation, and rapid nucleation kinetics. Because ssDNA is a flexible polymer, longer ssDNA can adopt more conformations and potentially reduce accessibility to nucleation sites that will initiate hybridization events and trigger liposome fusion. This is consistent with the observed decrease in fusion kinetics when the length of DNA receptors is 50 bp; however, this interpretation remains speculative at this time.

We also noted that fusion rates were universally lower for interfacial layers involving thicker PEG brushes, both in the absence of DNA receptors and even when one accounts for the relative sizes of DNA and PEG molecules. This suggests that the physical/mechanical properties of the PEG brush influence the mechanism of liposome fusion, beyond influencing the accessibility of the DNA. For example, a thicker PEG brush likely exerts a higher and broader repulsive free energy barrier that must be overcome either spontaneously (e.g., in the absence of DNA receptors), or during the "zippering up" component of DNA hybridization. Thus, we speculate that the mechanical properties of the interfacial PEG brush influence the overall liposome fusion rate by modulating the repulsive barrier that must be overcome in the *cis* DNA hybridization process.

Effects of DNA Availability on Liposome Fusion Kinetics. We found in previous work that DNA-mediated liposome fusion could be exploited for a molecular sensing platform.[12] This method incorporated aptamers, single-stranded DNA or RNA molecules that bind preselected targets with high specificity and selectivity,[43,44] as part of the detection scheme. DNA in the liposomes was engineered complementary to the aptamer sequence, so hybridization between liposome DNA and the aptamer prevented fusion with the liquid crystal unless a target analyte is present. Previous work looked at the presence of the aptamer sequence solely as a recognition element; however, the aptamer also serveed as a "blocking strand" in this system, preventing access to DNA in the

DOI: 10.1021/acsami.5b06351
ACS Appl. Mater. Interfaces 2015, 7, 20400−20409

liposome. Here, we aimed to increase sensitivity by modulating the concentration of the aptamer blocking strand.

To understand the effects of ssDNA availability on liposome fusion, we systematically varied the concentration of the blocking strand. Liposomes were prepared with 5′cholDNA (5′CHOL-Thr) that was complementary to a short (18 nucleotide), unfunctionalized oligomer (CS-Thr). When CS-Thr and 5′CHOL-Thr were present in solution at an equimolar ratio, we observed almost no liposome fusion at the interface (i.e., change in LC alignment) over the course of the experiment (Figure 3). The duplex form was thermodynamically favored at room temperature,[35] meaning that at any time, the vast majority of 5′cholDNA existed as a duplex with the complementary sequence (CS-Thr) and was therefore unable to hybridize with 3′cholDNA at the interface (3′CHOL-Thr) to trigger liposome fusion. A greater 5′CHOL-Thr/CS-Thr ratio resulted in significantly more rapid fusion kinetics, as more liposome DNA was left unblocked and was free to hybridize with DNA at the interface. When the ratio reached 4:1, we observed an immediate optical response from the LC. The liposome fusion rate (k_H > 1) corresponded to 50% homeotropic coverage on time scales <1 min. This was within error of experiments when no blocking strand was present and fusion proceeded immediately upon addition of liposomes. This experiment further confirmed that the accessibility of DNA receptor molecules played an important role in fusion kinetics, and the hybridization step in the fusion mechanism was successfully controlled by modulating the accessibility of the liposome DNA though the addition of a complementary blocking sequence.

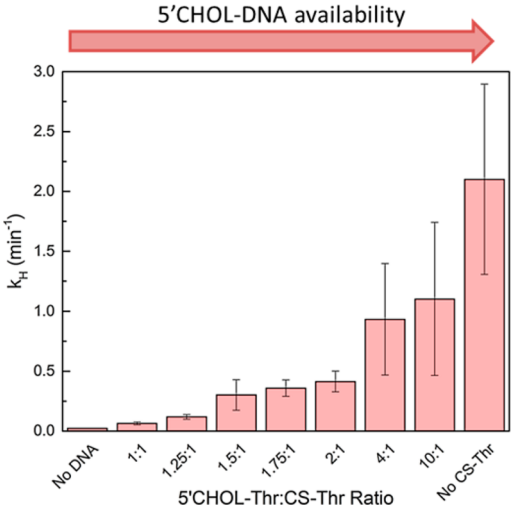

Figure 3. Liposome fusion rate in the presence of complementary blocking sequence. An increase in the ratio of cholesterol modified liposome DNA (5′CHOL-Thr) to blocking strand (CS-Thr) resulted in faster fusion kinetics as the availability of 5′CHOL-DNA increased.

Effects of Vesicle Composition on Liposome Fusion Kinetics. As mentioned above, it seems likely that the mechanical properties of the lipid bilayer of the liposome, for example, bending modulus and fluidity, would influence the kinetics of liposome rupture and fusion with the LC interface; both the spontaneous nonspecific fusion as well as the stress-induced fusion caused by cis hybridization of anchored DNA receptors. One way to test this hypothesis was to systematically vary the lipid composition of the liposomes in ways that affected these mechanical properties. Relevant factors include the degree of saturation of the hydrocarbon chains (unsaturated chains lead to greater bilayer fluidity),[45] the nature of the lipid headgroup (smaller headgroups reduce the bilayer stability and affect the bending modulus),[46] and the presence of sterol additives (e.g., cholesterol), which are believed to influence the rigidity of the bilayer.[47]

Interestingly, we found that a balance between saturated and unsaturated lipids, and lipids with large PC and small PE headgroups, was necessary to achieve rapid fusion kinetics. Figure 4 compares the receptor-mediated fusion of liposomes composed of either saturated DPPC or monounsaturated DOPC to liposomes containing a 50/50 mixture of saturated DPPC and unsaturated DOPE. Liposomes were prepared with either DPPC or DOPC and 5′CHOL-TG30 DNA (Table 1). The liposome dispersion was then introduced above a planar LC interface laden with DPSE-PEG1k and complementary 3′CHOL-AC30 DNA receptors. DNA-induced liposome fusion was monitored by the realignment of LC mesogens using polarized light microscopy. Liposomes composed of pure DPPC led to minimal LC realignment on time scales greater than 1 h (Figure 4A–C), as evident by small homeotropic domains that appeared in the LC film. Small defects in LC texture were observed along with changes in the birefringence colors, suggesting a change in the interfacial environment; however, liposomes did not rapidly fuse with the interface (indicated by the absence of large-scale LC reorientation). Similar results were observed when the liposomes were composed of unsaturated DOPC (Figure 4D–F). Interestingly, in the presence of mixed DOPC/DOPE liposomes (Figure 4G–I), an immediate and rapid LC response was observed (Figure 4G–I).

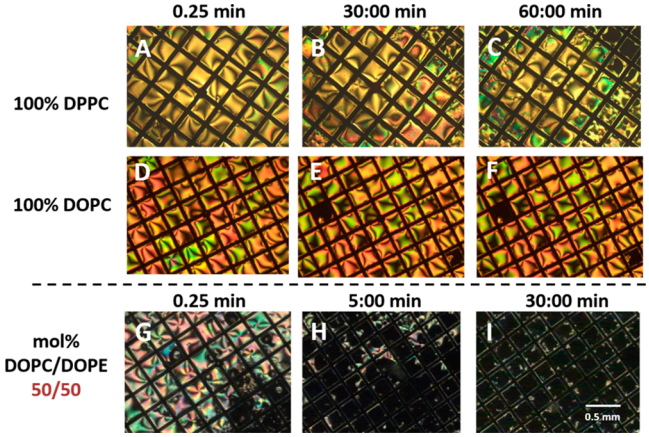

Figure 4. Polarized light microscopy images of the LC interface upon DNA-hybridization induced liposome fusion. Liposomes composed of pure DPPC (A–C) and DOPC (D–F) exhibited very slow fusion kinetics over the course of the hour-long experiment. However, liposomes prepared with a 50/50 mixture of the unsaturated lipids DOPC and DOPE resulted in an immediate response (G–I). Liposomes were added to a planar aligned LC interface at t = 0.

These results indicated that lipid composition was a critical factor in determining the fusion kinetics and suggested that PE headgroups and unsaturated chains were necessary to achieve significant rates of fusion. We hypothesized that these parameters, along with the cholesterol content, influenced the mechanical properties of the lipid bilayer (e.g., the bending modulus or mechanical stability), and that these three

DOI: 10.1021/acsami.5b06351
ACS Appl. Mater. Interfaces 2015, 7, 20400–20409

components (i.e., degree of unsaturation, headgroup size, and cholesterol content) would have a major impact on the destabilization and rupture of liposome at the interface. In the study below, we examined the effect of headgroup, lipid chain saturation, and cholesterol content on DNA-induced liposome fusion with the LC interface.

To examine this hypothesis in greater detail, we explored the effects of composition systematically, starting with the influence of the PE headgroup. DOPE is known to destabilize bilayers due to the inverted cone shape of the molecule and its tendency to form nonlamellar phases in aqueous solution.[46,48,49] An increase in the DOPE content of the liposomes was therefore expected to lead to faster fusion kinetics. As shown in Figure 5A–D, liposomes composed of pure DOPC added to the

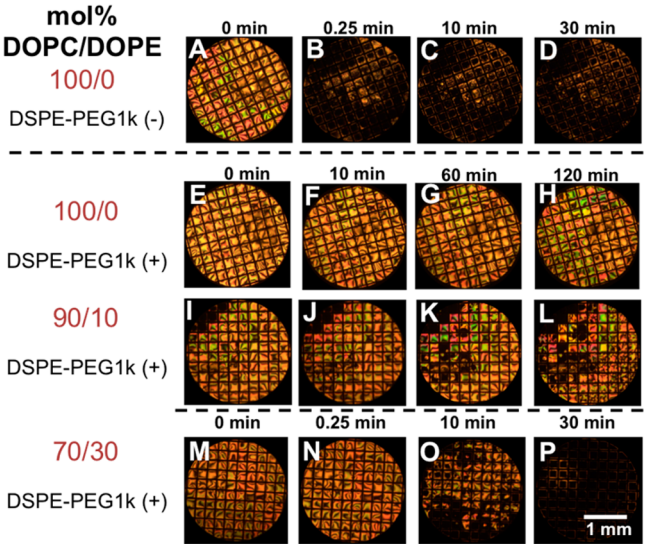

Figure 5. Polarized light microscopy images of the LC interface with liposomes containing DOPE. LC reorientation is observed when liposomes are added to an interface (A–D) without DSPE-PEG1k to prevent spontaneous fusion. DNA hybridization-induced liposome fusion is observed when the mol % DOPE exceeds 30% (M–P), but is not present on applicable time scales when the mol % DOPE is 0 (E–H) or 10% (I–L).

aqueous phase above a *bare* LC interface (i.e., DSPE-PEG1k lipids were not present to create a steric barrier) immediately fused and realigned the sample as expected due to nonspecific vesicle fusion. However, when the steric barrier was present (Figure 5E–H), the same DOPC liposomes showed no evidence of fusion, even in the presence of complementary DNA receptors at both interfaces. Small homeotropic domains appeared when the liposomes contained 10 mol % DOPE (Figure 5I–L), but liposomes did not fuse with the interface at short incubation times until the concentration of DOPE exceeded 30 mol % (Figure 5M–P).

To quantify the effects of liposome DOPE content on fusion kinetics, we determined an effective rate constant for each lipid mixture. As shown in Figure 6, increasing the mol % DOPE content in mixed DOPC/DOPE liposomes led to a faster rate of DNA-induced fusion. Nonspecific fusion events, where no DNA was present and fusion events occurred by the spontaneous adsorption of liposomes that penetrated the steric barrier, also increased with DOPE content. High concentrations of DOPE (>40 mol %) caused a large number of nonspecific fusion events, leading to LC reorientation on the

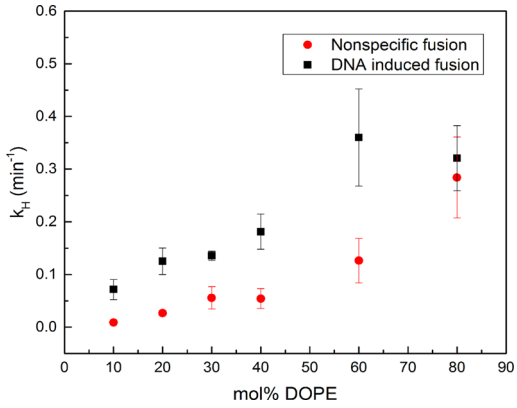

Figure 6. Effective rate constant of DNA-hybridization induced fusion with increasing DOPE content in mixed DOPE/DOPC liposomes. The effective rate constant (k_H) was defined as the inverse time to reach 50% homeotropic coverage.

order of minutes. In particular, at a composition of 80% DOPE, the time scale for nonspecific fusion was nearly identical to that of DNA-induced fusion. These results indicated that liposomes containing a 40:60 DOPE/DOPC mixture represented a good compromise to achieve both rapid DNA-induced fusion and slow nonspecific fusion.

On the basis of these findings, DOPE was determined to be a critical liposome component to facilitate fusion. DOPE is commonly utilized in cationic liposomes to increase transfection efficiency, as it has a high propensity to transition to the nonlamellar H_{II} phase.[50−52] The same molecular properties also contribute to bilayer destabilization and, in our system, an increased rate of vesicle rupture at the LC interface. However, both receptor-mediated and nonspecific fusion were increased by the presence of high concentrations of DOPE, suggesting that bilayer stress induced by DNA-hybridization was no longer a necessary step in the fusion mechanism when DOPE content was large. Moreover, since DOPE comprises unsaturated chains and a small PE headgroup, it was not clear which of these two structural features was responsible for the effects on fusion kinetics. In order to address these issues, we aimed to modulate the fluidity and flexibility of the bilayer independent of the stability of the system. We hypothesized that fusion kinetics could be modulated by controlling bilayer fluidity though the degree of unsaturation and cholesterol content of the liposomes.

To directly investigate the effect of lipid saturation on the fusion kinetics, we held the DOPE content of the liposome constant at 30 mol % (the minimum necessary to achieve significant fusion), and systematically varied the ratio of saturated to unsaturated PC lipid. DPPC and DOPC share a large choline headgroup but vary in the degree of unsaturation in their lipid tails. DPPC lipids are fully saturated and arrange into tightly packed tilted chains at room temperature, while DOPC, with two monounsaturated chains, exists in a fluid-like liquid crystalline phase at room temperature. Because DOPC chains pack poorly, we expected to observe faster fusion kinetics when DOPC represented a larger percentage of the liposome composition. Figure 7A shows a dramatic and systematic increase in the rate of DNA-mediated liposome fusion with an increase in the unsaturated lipid content. Notably, the extent of nonspecific fusion increased only minimally, and at high DOPC fractions the DNA-mediated fusion was more than an order of magnitude faster than

DOI: 10.1021/acsami.5b06351
ACS Appl. Mater. Interfaces 2015, 7, 20400−20409

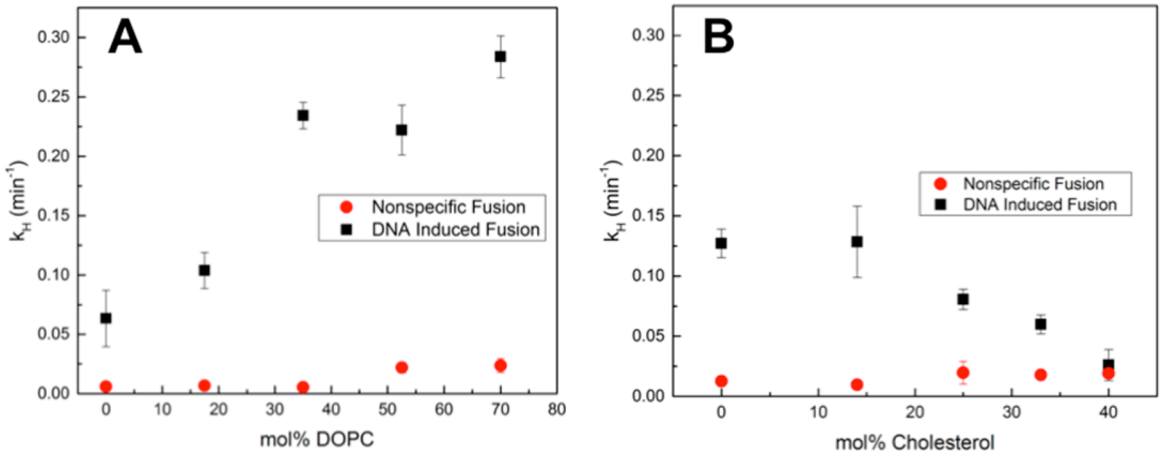

Figure 7. Liposome composition effects on kinetics of LC realignment. The effective rate constants (k_H) for DNA hybridization induced fusion at the LC interface for increasing content of (A) DOPC and (B) cholesterol. Liposomes in (A) contained 30 mol % DOPE to promote DNA-mediated fusion and a varying ratio of DOPC/DPPC, while liposomes in (B) contained a fixed 2:1 molar ratio of DOPC/DOPE.

nonspecific fusion. Vesicles prepared with unsaturated lipids presumably exhibited a more fluid and flexible bilayer, which ruptured more readily under bilayer stress (i.e., cis DNA hybridization events). However, the high fraction of PC lipids resulted in highly stable liposomes that did not fuse readily in the absence of DNA hybridization.

Lastly, we explored the effect of cholesterol on the fusion kinetics of our system. Cholesterol is an important component of biological membranes, reducing membrane permeability,[53] influencing the lateral movement of lipids and proteins,[54] and modulating the acyl-chain packing order and fluidity.[55] In our system of unsaturated lipids in the liquid crystalline phase cholesterol serves to increase bilayer rigidity and decrease permeability through the condensing effect, reducing the area per molecule and thickening the bilayer.[56,57] We hypothesized that the presence of cholesterol would reduce fluctuations that lead to hydrophobic interactions between lipid tails and the LC interface upon vesicle strain, stabilizing the liposome and slowing fusion kinetics. Liposomes were prepared with at 2:1 molar ratio of DOPC/DOPE, and cholesterol was incorporated to create a three component system. We observed a reduction in the rate of DNA-mediated fusion upon increased cholesterol content (Figure 7B), particularly above 20 mol % cholesterol. The rate of nonspecific fusion was relatively insensitive to cholesterol content.

The physical and mechanical properties of cholesterol-containing lipid bilayers have been extensively studied,[47,58−64] and both lipid headgroup and degree of unsaturation play a role in governing these complex interactions. The presence of cholesterol in our system was empirically found to reduce the liposome fusion rate, and we hypothesize that a decrease in bilayer permeability contributed to the slower kinetics. Evidence has shown that cholesterol interacts more strongly with saturated lipids than those with double bonds.[61] Interestingly, cholesterol does not affect the bending rigidity of unsaturated membranes; however, the bending modulus dramatically increases when cholesterol is a component of bilayers with saturated lipids.[62,63] This would suggest that in our system of unsaturated lipids, bilayer flexibility did not contribute to the observed decrease in fusion rates associated with cholesterol content. It is likely that cholesterol decreased permeability of the liposome by its ability to "fill-in" between the poorly packed chains (which contain cis-double bonds) in the unsaturated lipid bilayer. In this scenario, cholesterol may limit the exposure of hydrophobic lipid tails under DNA-induced stress and reduce the hydrophobic effect and attractive forces between exposed tails and the LC. However, the role of cholesterol in membrane dynamics is complex and we refrain from speculating further on its influence on our system since our macroscopic observations of liposome fusion provide limited molecular-level insight.

Experimental evidence showed that liposomes composed of DOPC, DPPC and DOPE were an ideal formulation for fast receptor-mediated liposome fusion at the aqueous−LC interface. They provided rapid fusion kinetics ($k_H > 0.2$ min^{-1}) with little to no nonspecific fusion. These three components modulated the mechanical properties of the bilayer, which allowed us to tune the overall stability of the system and trigger rapid DNA-induced fusion while inhibiting nonspecific fusion. The presence of unsaturated lipids increased the rate of fusion, presumably by preventing lipid close-packing and increasing disorder in the membrane. DOPE was found to be a particularly important component because, consistent with its ability to exhibit inverted hexagonal phases,[65] it destabilized the bilayer and promoted fusion events. It is likely that cholesterol decreased the rate of fusion by reducing membrane permeability and hydrophobic attractive forces between the lipid tails and the liquid crystal. All of these parameters contributed to the overall bilayer stability and controlled how liposome behavior under mechanical stress (i.e., cis DNA-hybridization events inducing strain on the bilayer). Although we have shown that cholesterol can be used to modify fusion kinetics, its incorporation into the bilayer resulted in slower fusion kinetics overall and was not ideal for our sensing platform. Liposomes prepared with roughly equimolar amounts of DOPC/DPPC/DOPE lipids experimentally allowed for rapid DNA-induced vesicle fusion with low nonspecific fusion at the liquid crystal interface.

CONCLUSIONS

Interfacial liposome fusion is an important biomimetic process that can be studied through observation of liquid crystal orientation. In this work, we have systematically studied the molecular variables that govern liposome fusion to advance understanding of the fusion mechanism and the importance of individual contributing parameters. The knowledge gained here

DOI: 10.1021/acsami.5b06351
ACS Appl. Mater. Interfaces 2015, 7, 20400−20409

can be applied to numerous drug delivery, bioassay, and biosensing platforms by enhancing the sensitivity, selectivity, and robustness of the system. For example, we have shown that these principles can be applied to improve the kinetics and sensitivity of a biosensing platform based on programmed liposome fusion at LC interfaces.[12] Fusion kinetics can be modulated by controlling the accessibility of DNA at the interface through DNA length and PEG headgroup size. Lipid composition also played an important role in the dynamics of vesicle rupture at the interface. The composition was used to modulate mechanical properties of the bilayer (e.g., bending modulus, fluidity, and permeability) to facilitate fusion events under DNA-hybridization induced stress. Liposomes composed of a mixture of saturated (DPPC) and unsaturated (DOPC/DOPE) lipids resulted in the rapid fusion kinetics (k_H > 0.2 min^{-1}) and minimal nonspecific fusion events crucial for the implementation of controlled fusogenic systems in drug delivery, gene transfer, and sensing platforms.

AUTHOR INFORMATION

Corresponding Author

*E-mail: daniel.schwartz@colorado.edu.

Notes

The authors declare no competing financial interest.

ACKNOWLEDGMENTS

The authors gratefully acknowledge support from the National Science Foundation award (CBET-1160202) and from the Soft Materials Research Center (NSF-MRSEC DMR 1420736). K.M.M. acknowledges support through a Department of Education GAANN fellowship (GAANN ED P200A120014).

REFERENCES

(1) Oren-Suissa, M.; Podbilewicz, B. Cell Fusion During Development. *Trends Cell Biol.* **2007**, *17* (11), 537−546.

(2) Ungar, D.; Hughson, F. M. SNARE Protein Structure and Function. *Annu. Rev. Cell Dev. Biol.* **2003**, *19*, 493−517.

(3) Hoppins, S.; Lackner, L.; Nunnari, J. The Machines that Divide and Fuse Mitochondria. *Annu. Rev. Biochem.* **2007**, *76*, 751−780.

(4) Skehel, J. J.; Wiley, D. C. Receptor Binding and Membrane Fusion in Virus Entry: The Inflenza Hemagglutinin. *Annu. Rev. Biochem.* **2000**, *69*, 531−49.

(5) Marsden, H. R.; Tomatsu, I.; Kros, A. Model Systems for Membrane Fusion. *Chem. Soc. Rev.* **2011**, *40* (3), 1572−1585.

(6) Ma, M.; Bong, D. Controlled Fusion of Synthetic Lipid Membrane Vesicles. *Acc. Chem. Res.* **2013**, *46* (12), 2988−2997.

(7) Smith, E. A.; Weisshaar, J. C. Docking, not fusion, as the rate-limiting step in a SNARE-driven vesicle fusion assay. *Biophys. J.* **2011**, *100* (9), 2141−50.

(8) Fix, M.; Melia, T. J.; Jaiswal, J. K.; Rappoport, J. Z.; You, D.; Sollner, T. H.; Rothman, J. E.; Simon, S. M. Imaging single membrane fusion events mediated by SNARE proteins. *Proc. Natl. Acad. Sci. U. S. A.* **2004**, *101* (19), 7311−7316.

(9) Pahler, G.; Panse, C.; Diederichsen, U.; Janshoff, A. Coiled-coil formation on lipid bilayers–implications for docking and fusion efficiency. *Biophys. J.* **2012**, *103* (11), 2295−2303.

(10) Stengel, G.; Zahn, R.; Höök, F. DNA-Induced Programmable Fusion of Phospholipid Vesicles. *J. Am. Chem. Soc.* **2007**, *129*, 9584−9585.

(11) Chan, Y. H.; Lenz, P.; Boxer, S. G. Kinetics of DNA-mediated docking reactions between vesicles tethered to supported lipid bilayers. *Proc. Natl. Acad. Sci. U. S. A.* **2007**, *104* (48), 18913−18918.

(12) Noonan, P. S.; Mohan, P.; Goodwin, A. P.; Schwartz, D. K. DNA Hybridization-Mediated Liposome Fusion at the Aqueous Liquid Crystal Interface. *Adv. Funct. Mater.* **2014**, *24* (21), 3206−3212.

(13) Mohan, P.; Noonan, P. S.; Nakatsuka, M. A.; Goodwin, A. P. On-Demand Droplet Fusion: A Strategy for Stimulus-Responsive Biosensing in Solution. *Langmuir* **2014**, *30*, 12321−12327.

(14) Pattni, B. S.; Chupin, V. V.; Torchilin, V. P. New Developments in Liposomal Drug Delivery. *Chem. Rev.* **2015**, DOI: 10.1021/acs.chemrev.5b00046.

(15) Huang, S.-L. Liposomes in Ultrasonic Drug and Gene Delivery. *Adv. Drug Delivery Rev.* **2008**, *60*, 1167−1176.

(16) Bai, Y.; Abbott, N. L. Recent Advances in Colloidal and Interfacial Phenomena Involving Liquid Crystals. *Langmuir* **2011**, *27* (10), 5719−5738.

(17) Dunmur, D.; Toriyama, K.; Demus, D.; Goodby, J.; Gray, G. W.; Spiess, H.-W.; Vill, V. *Handbook of Liquid Crystals*, Vol. *1*; Wiley-VCH Verlag GmbH: Weinheim, Germany, 1998.

(18) Walba, D. M.; Liberko, C. A.; Korblova, E.; Farrow, M.; Furtak, T. E.; Chow, B. C.; Schwartz, D. K.; Freeman, A. S.; Douglas, K.; Williams, S. D.; Klittnick, A. F.; Clark, N. A. Self-Assembled Monolayers for Liquid Crystal Alignment: Simple Preparation on Glass Using Alkyltrialkoxysilanes. *Liq. Cryst.* **2004**, *31* (4), 481−489.

(19) Noonan, P. S.; Shavit, A.; Acharya, B. R.; Schwartz, D. K. Mixed Alkylsilane Functionalized Surfaces for Simultaneous Wetting and Homeotropic Anchoring of Liquid Crystals. *ACS Appl. Mater. Interfaces* **2011**, *3* (11), 4374−4380.

(20) Brake, J. M.; Abbott, N. L. An Experimental System for Imaging the Reversible Adsorption of Amphiphiles at Aqueous-Liquid Crystal Interfaces. *Langmuir* **2002**, *18*, 6101−6109.

(21) Brake, J. M.; Mezera, A. D.; Abbott, N. L. Effect of Surfactant Structure on the Orientation of Liquid Crystals at Aqueous-Liquid Crystal Interfaces. *Langmuir* **2003**, *19* (16), 6436−6442.

(22) McUmber, A. C.; Noonan, P. S.; Schwartz, D. K. Surfactant−DNA Interactions at the Liquid Crystal−Aqueous Interface. *Soft Matter* **2012**, *8* (16), 4335−4342.

(23) Uline, M. J.; Meng, S.; Szleifer, I. Surfactant Driven Surface Anchoring Transitions in Liquid Crystal Thin Films. *Soft Matter* **2010**, *6* (21), 5482−5490.

(24) Lockwood, N.; Abbott, N. Self-Assembly of Surfactants and Phospholipids at Interfaces between Aqueous Phases and Thermotropic Liquid Crystals. *Curr. Opin. Colloid Interface Sci.* **2005**, *10* (3−4), 111−120.

(25) Price, A. D.; Schwartz, D. K. Fatty-Acid Monolayers at the Nematic/Water Interface: Phases and Liquid-Crystal Alignment. *J. Phys. Chem. B* **2007**, *111* (5), 1007−1015.

(26) Brake, J. M.; Daschner, M. K.; Luk, Y. Y.; Abbott, N. L. Biomolecular Interactions at Phospholipid-Decorated Surfaces of Liquid Crystals. *Science* **2003**, *302* (5653), 2094−2097.

(27) Brake, J. M.; Daschner, M. K.; Abbott, N. L. Formation and Characterization of Phospholipid Monolayers Spontaneously Assembled at Interfaces between Aqueous Phases and Thermotropic Liquid Crystals. *Langmuir* **2005**, *21* (6), 2218−2228.

(28) Sofia, S. J.; Premnath, V.; Merrill, E. W. Poly(ethylene oxide) Grafted to Silicon Surfaces: Grafting Density and Protein Adsorption. *Macromolecules* **1998**, *31* (15), 5059−5070.

(29) Meli, M. V.; Lin, I.-H.; Abbott, N. L. Preparation of Microscopic and Planar Oil-Water Interfaces That Are Decorated with Prescribed Densities of Insoluble Amphiphiles. *J. Am. Chem. Soc.* **2008**, *130* (13), 4326−4333.

(30) Chan, Y. H.; van Lengerich, B.; Boxer, S. G. Lipid-Anchored DNA Mediates Vesicle Fusion as Observed by Lipid and Content Mixing. *Biointerphases* **2008**, *3* (2), FA17−FA21.

(31) Kinsinger, M. I.; Lynn, D. M.; Abbott, N. L. Nematic Ordering Drives the Phase Separation of Mixed Monolayers Containing Phospholipids Modified with poly(ethylene glycol) at Aqueous−Liquid Crystal Interfaces. *Soft Matter* **2010**, *6* (17), 4095−4104.

(32) van Lengerich, B.; Rawle, R. J.; Bendix, P. M.; Boxer, S. G. Individual vesicle fusion events mediated by lipid-anchored DNA. *Biophys. J.* **2013**, *105* (2), 409−19.

(33) Devanand, K.; Selser, J. C. Asymptotic Behavior and Long-Range Interactions in Aqueous Solutions of Poly(ethy1ene oxide). *Macromolecules* **1991**, *24* (22), 5943−5947.

DOI: 10.1021/acsami.5b06351
ACS Appl. Mater. Interfaces 2015, 7, 20400−20409

(34) Sim, A. Y. L.; Lipfert, J.; Herschlag, D.; Doniach, S. Salt Dependence of the Radius of Gyration and Flexibility of Single-Stranded DNA in Solution Probed by Small-Angle X-ray Scattering. *Phys. Rev. E: Stat., Nonlinear, Soft Matter Phys.* **2012**, *86* (2), 021901.
(35) Bloomfield, V. A.; Crothers, D. M.; Tinoco, I. *Nucleic Acids: Structures, Properties, and Functions*; University Science Books: Sausalito, CA, 2000.
(36) Chen, C.; Wang, W.; Wang, Z.; Wei, F.; Zhao, X. S. Influence of Secondary Structure on Kinetics and Reaction Mechanism of DNA Hybridization. *Nucleic Acids Res.* **2007**, *35* (9), 2875−2884.
(37) Pörschke, D.; Eigen, M. Co-operative Non-enzymic Base Recognition III. Kinetics of the Helix-Coil Transition of the Oligoribouridylic-Oligoboadenylic Acid System and of Oligoriboadenylic Acid alone at Acidic pH. *J. Mol. Biol.* **1971**, *62*, 361−381.
(38) Jo, J. J.; Kim, M. J.; Son, J. T.; Kim, J.; Shin, J. S. Single-Fluorophore Monitoring of DNA Hybridization for Investigating the Effect of Secondary Structure on the Nucleation Step. *Biochem. Biophys. Res. Commun.* **2009**, *385* (1), 88−93.
(39) Peterson, A. W.; Heaton, R. J.; Georgiadis, R. M. The Effect of Surface Probe Density on DNA Hybridization. *Nucleic Acids Res.* **2001**, *29* (24), 5163−5168.
(40) Peterson, A. W.; Wolf, L. K.; Georgiadis, R. M. Hybridization of Mismatched or Partially Matched DNA at Surfaces. *J. Am. Chem. Soc.* **2002**, *124* (49), 14601−14607.
(41) Monserund, J. H.; Schwartz, D. K. Mechanisms of Surface-Mediated DNA Hybridization. *ACS Nano* **2014**, *8* (5), 4488−4499.
(42) Okahata, Y.; Kawase, M.; Niikura, K.; Ohtake, F.; Furusawa, H.; Ebara, Y. Kinetic Measurements of DNA Hybridization on an Oligonucleotide-Immobilized 27-MHz Quartz Crystal Microbalance. *Anal. Chem.* **1998**, *70* (7), 1288−1296.
(43) Tuerk, C.; Gold, L. Systematic Evolution of Ligands by Exponential Enrichment: RNA Ligands to Bacteriophage T4 DNA Polymerase. *Science* **1990**, *249*, 505−510.
(44) Ellington, A. D.; Szostak, J. W. In vitro Selection of RNA Molecules that Bind Specific Ligands. *Nature* **1990**, *346*, 818−822.
(45) Svetlovics, J. A.; Wheaten, S. A.; Almeida, P. F. Phase Separation and Fluctuations in Mixtures of a Saturated and an Unsaturated Phospholipid. *Biophys. J.* **2012**, *102* (11), 2526−2535.
(46) Siegel, D. P.; Epand, R. M. The Mechanism of Lamellar-to-Inverted Hexagonal Phase Transitions in Phosphatidylethanolamine: Implications for Membrane Fusion Mechanisms. *Biophys. J.* **1997**, *73*, 3089−3111.
(47) Chen, Z.; Rand, R. P. The Influence of Cholesterol on Phospholipid Membrane Curvature and Bending Elasticity. *Biophys. J.* **1997**, *73*, 267−276.
(48) Holopainen, J. M.; Lehtonen, J. Y. A.; Kinnunen, P. K. J. Evidence for the Extended Phospholipid Conformation in Membrane Fusion and Hemifusion. *Biophys. J.* **1999**, *76*, 2111−2120.
(49) Ellens, H.; Siegel, D. P.; Alford, D.; Yeagle, P. L.; Boni, L.; Lis, L. J.; Quinn, P. J.; Bentz, J. Membrane Fusion and Inverted Phases. *Biochemistry* **1989**, *28* (9), 3692−3703.
(50) Rand, R. P.; Fuller, N. L.; Gruner, S. M.; Parsegian, V. A. Membrane Curvature, Lipid Segregation, and Structural Transitions for Phospholipids under Dual-Solvent Stress. *Biochemistry* **1990**, *29* (1), 76−87.
(51) McIntosh, T. J. Hydration Properties of Lamellar and Non-Lamellar Phases of Phosphatidylcholine and Phosphatidylethanolamine. *Chem. Phys. Lipids* **1996**, *81*, 117−131.
(52) Ma, B.; Zhang, S.; Jiang, H.; Zhao, B.; Lv, H. Lipoplex Morphologies and Their Influences on Transfection Efficiency in Gene Delivery. *J. Controlled Release* **2007**, *123* (3), 184−194.
(53) De Gier, J.; Mandersloot, J. G.; Van Deenen, L. L. M. Lipid Composition and Permeability of Liposomes. *Biochim. Biophys. Acta, Biomembr.* **1968**, *150*, 666−675.
(54) Kwik, J.; Boyle, S.; Fooksman, D.; Margolis, L.; Sheetz, M. P.; Edidin, M. Membrane Cholesterol, Lateral Mobility, and the Phosphatidylinositol 4,5-bisphosphate-dependent Organization of Cell Actin. *Proc. Natl. Acad. Sci. U. S. A.* **2003**, *100* (24), 13964−13969.
(55) Yeagle, P. L. Cholesterol and the Cell Membrane. *Biochim. Biophys. Acta, Rev. Biomembr.* **1985**, *822*, 267−287.
(56) Hung, W. C.; Lee, M. T.; Chen, F. Y.; Huang, H. W. The Condensing Effect of Cholesterol in Lipid Bilayers. *Biophys. J.* **2007**, *92* (11), 3960−3967.
(57) de Meyer, F.; Smit, B. Effect of Cholesterol on the Structure of a Phospholipid Bilayer. *Proc. Natl. Acad. Sci. U. S. A.* **2009**, *106* (10), 3654−3658.
(58) Simon, S. A.; McIntosh, T. J.; Latorre, R. Influence of Cholesterol on Water Penetration into Bilayers. *Science* **1982**, *216* (2), 65−67.
(59) Rukmini, R.; Rawat, S. S.; Biswas, S. C.; Chattopadhyay, A. Cholesterol Organization in Membranes at Low Concentrations: Effects of Curvature Stress and Membrane Thickness. *Biophys. J.* **2001**, *81* (4), 2122−2134.
(60) Henriksen, J.; Rowat, A. C.; Brief, E.; Hsueh, Y. W.; Thewalt, J. L.; Zuckermann, M. J.; Ipsen, J. H. Universal Behavior of Membranes with Sterols. *Biophys. J.* **2006**, *90* (5), 1639−1649.
(61) Pan, J.; Mills, T.; Tristram-Nagle, S.; Nagle, J. Cholesterol Perturbs Lipid Bilayers Nonuniversally. *Phys. Rev. Lett.* **2008**, *100* (19), 198103.
(62) Pan, J.; Tristram-Nagle, S.; Nagle, J. Effect of Cholesterol on Structural and Mechanical Properties of Membranes Depends on Lipid Chain Saturation. *Phys. Rev. E: Stat., Nonlinear, Soft Matter Phys.* **2009**, *80* (2), 021931.
(63) Gracià, R. S.; Bezlyepkina, N.; Knorr, R. L.; Lipowsky, R.; Dimova, R. Effect of Cholesterol on the Rigidity of Saturated and Unsaturated Membranes: Fluctuation and Electrodeformation Analysis of Giant Vesicles. *Soft Matter* **2010**, *6* (7), 1472−1482.
(64) Khelashvili, G.; Johner, N.; Zhao, G.; Harries, D.; Scott, H. L. Molecular Origins of Bending Rigidity in Lipids with Isolated and Conjugated Double Bonds: The Effect of Cholesterol. *Chem. Phys. Lipids* **2014**, *178*, 18−26.
(65) Marrink, S. J.; Mark, A. E. Molecular View of Hexagonal Phase Formation in Phospholipid Membranes. *Biophys. J.* **2004**, *87* (6), 3894−3900.

DOI: 10.1021/acsami.5b06351
ACS Appl. Mater. Interfaces 2015, 7, 20400−20409